Published OnlineFirst August 3, 2020; DOI: 10.1158/1535-7163.MCT-20-0237

PF-06804103, A Site-specific Anti-HER2 Antibody–Drug Conjugate for the Treatment of HER2-expressing Breast, Gastric, and Lung Cancers

Edmund I. Graziani[1], Matthew Sung[2], Dangshe Ma[2], Bitha Narayanan[2], Kimberly Marquette[3], Sujiet Puthenveetil[1], L. Nathan Tumey[1], Jack Bikker[1], Jeffrey Casavant[1], Eric M. Bennett[3], Manoj B. Charati[2], Jonathon Golas[2], Christine Hosselet[2], Cynthia M. Rohde[4], George Hu[4], Magali Guffroy[4], Hadi Falahatpisheh[4], Martin Finkelstein[4], Tracey Clark[5], Frank Barletta[6], Lioudmila Tchistiakova[3], Judy Lucas[2], Edward Rosfjord[2], Frank Loganzo[2], Christopher J. O'Donnell[1], Hans-Peter Gerber[2], and Puja Sapra[2]

ABSTRACT

The approval of ado-trastuzumab emtansine (T-DM1) in HER2$^+$ metastatic breast cancer validated HER2 as a target for HER2-specific antibody–drug conjugates (ADC). Despite its demonstrated clinical efficacy, certain inherent properties within T-DM1 hamper this compound from achieving the full potential of targeting HER2-expressing solid tumors with ADCs. Here, we detail the discovery of PF-06804103, an anti-HER2 ADC designed to have a widened therapeutic window compared with T-DM1. We utilized an empirical conjugation site screening campaign to identify the engineered kK183C and K290C residues as those that maximized *in vivo* ADC stability, efficacy, and safety for a four drug–antibody ratio (DAR) ADC with this linker–payload combination. PF-06804103 incorporates the following novel design elements: (i) a new auristatin payload with optimized pharmacodynamic properties, (ii) a cleavable linker for optimized payload release and enhanced antitumor efficacy, and (iii) an engineered cysteine site–specific conjugation approach that overcomes the traditional safety liabilities of conventional conjugates and generates a homogenous drug product with a DAR of 4. PF-06804103 shows (i) an enhanced efficacy against low HER2-expressing breast, gastric, and lung tumor models, (ii) overcomes *in vitro*- and *in vivo*–acquired T-DM1 resistance, and (iii) an improved safety profile by enhancing ADC stability, pharmacokinetic parameters, and reducing off-target toxicities. Herein, we showcase our platform approach in optimizing ADC design, resulting in the generation of the anti-HER2 ADC, PF-06804103. The design elements of identifying novel sites of conjugation employed in this study serve as a platform for developing optimized ADCs against other tumor-specific targets.

Introduction

Antibody–drug conjugates (ADC) are established therapeutic modalities that aim to selectively deliver chemotherapeutic agents to tumors while limiting nontumor tissue toxicities (1). Anticancer ADCs are comprised of a tumor-targeting antibody attached to a cytotoxic payload via a chemical linker. Following binding to a tumor-specific surface antigen, the ADC is internalized into tumor cells where the chemical linker is processed, and the cytotoxic payload is released. Following the first approval of gemtuzumab ozogamicin, seven other ADCs (ado-trastuzumab emtansine, brentuximab vedotin, inotuzumab ozogamicin, polatuzumab vedotin, trastuzumab deruxtecan, enfortumab vedotin, and sacituzumab govitecan) have garnered FDA approval, sparking industry-wide interest in this modality with approximately 80 ADCs now in clinical development (2, 3). However, clinical development of many of these ADCs was halted because of their limited therapeutic window. Thus, efforts to widen the therapeutic window of ADCs have led to the optimization of their modular components including antibody structure, conjugation chemistries, and payload diversification (3).

T-DM1 is comprised of the anti-HER2 antibody, trastuzumab, conjugated to the maytansinoid emtansine (DM1) via a noncleavable thioether linkage (mcc-DM1; ref. 4). Brentuximab vedotin is comprised of an anti-CD30 antibody conjugated to the auristatin monomethyl auristatin E (MMAE) via the enzymatically cleavable valine-citrulline dipeptide linkage (vc-MMAE; ref. 5). Many of the ADCs in clinical evaluation utilize the same linker–payload and conjugation chemistry as brentuximab vedotin. Despite targeting different antigens, ADCs that employ these linker–payloads have similar MTDs, which are driven by the same off-target dose-limiting toxicities (DLT) in patients with cancer (6). It is likely that at the MTD for these ADCs, most patients may not achieve the local tumor exposure of the cytotoxic payload necessary for meaningful clinical benefit (6). The mechanism responsible for these off-target DLTs is not fully elucidated; however, we and others hypothesize that ADC instability and premature payload release into the circulation may be the primary attribute responsible for the MTDs and DLTs reported for these ADCs (6).

[1]Pfizer Inc., World Wide Medicinal Chemistry, Groton, Connecticut. [2]Pfizer Inc., Oncology Research & Development, Pearl River, New York. [3]Pfizer Inc., BioMedicine Design, Cambridge, Massachusetts. [4]Pfizer Inc., Drug Safety Research & Development, Pearl River, New York. [5]Pfizer Inc., BioMedicine Design, Groton, Connecticut. [6]Pfizer Inc., BioMedicine Design, Pearl River, New York.

Note: Supplementary data for this article are available at Molecular Cancer Therapeutics Online (http://mct.aacrjournals.org/).

E.I. Graziani and M. Sung contributed equally as co-first authors of this article.

Corresponding Authors: Matthew Sung, Pfizer, Inc., 401 N. Middletown Road, 200/4214, Pearl River, NY 10965. Phone: 317-902-2491; Fax: 845-474-3161; E-mail: sungms@gmail.com; and Puja Sapra, Pfizer, Inc., 401 N. Middletown Road, Phone: 845-608-3303; E-mail: Psapra111@gmail.com.

Mol Cancer Ther 2020;19:2068–78

doi: 10.1158/1535-7163.MCT-20-0237

Various site-specific conjugation approaches have been explored to enhance ADC stability. The THIOMAB approach used surface-exposed cysteines engineered into the antibody backbone specifically conjugated to the linker–payload that resulted in a homogenous drug product, an improved pharmacokinetic profile, and expanded therapeutic window for these ADCs (7). Engineering nonnative amino acid residues into the antibody led to a similar pharmacologic profile (8). These approaches for optimizing site-specific conjugation have focused on generating drug–antibody ratios (DAR) equivalent to 2. We recently reported on the various physicochemical factors that influence optimal valine-citrulline linker–payload conjugation site selection with respect to the stability of 2 DAR ADCs (9). These reports demonstrate that the location of conjugation site influences ADC stability, and the molecular nature of different linker–payloads dictates which sites are optimal for each linker–payload combination.

HER2 is an attractive target for ADC development in oncology as the protein is enriched in a variety of solid tumor indications including breast, gastric, non–small cell lung cancer, etc. (10). Given the modular nature of ADCs, a diverse set of approaches has been undertaken to develop anti-HER2 ADCs with different properties to address the limited clinical efficacy of T-DM1 (11). SYD985 is comprised of trastuzumab conventionally conjugated to a valine-citrulline linker with a duocarmycin (DNA targeting) payload (∼2.8 DAR; ref. 12). ARX788 is comprised of an engineered anti-HER2 antibody containing an unnatural amino acid linker, para-acetyl-phenylalanine, that enables site-specific conjugation of the dolastatin monomethyl auristatin F (microtubule targeting) payload (1.9 DAR; ref. 13). MEDI2476 is composed of a biparatopic anti-HER2 antibody targeting two different epitopes in the HER2 protein, site specifically conjugated via a maleimidocaproyl linker to a tubulysin payload (4 DAR; ref. 14). DS-8201a (trastuzumab deruxtecan) is composed of trastuzumab conventionally conjugated to DXd payload (topoisomerase I targeting) via an enzymatically cleavable maleimide glycyn-glycyn-phenylalanyn-glycyn peptide linker (7–8 DAR; ref. 15). These, and other, anti-HER2 ADCs have shown better efficacy than T-DM1 in preclinical tumor models and are currently being explored for clinical benefit in patients with HER2-expressing tumors.

Herein, we describe our platform approach utilizing antibody engineering and site-specific conjugation to generate an anti-HER2 ADC with an optimized therapeutic window compared with T-DM1. We hypothesized that certain conjugation sites of the linker–payload affect *in vivo* ADC stability, and set out to identify a combination of sites that would lead to an ADC with an efficacy, stability, and safety profile suitable for the treatment of HER2-expressing cancers. The auristatin microtubule inhibitor, Aur0101 (16), was conjugated to engineered cysteines in an anti-HER2 antibody backbone via a valine-citrulline linker ("vc0101") with a target DAR of 4, to develop the anti-HER2 ADC candidate molecule, PF-06804103. This work highlights the concept that not all sites within the antibody framework are created equal for the site-specific conjugation approach to the ADC platform. Thus, for every linker–payload combination, an empirical approach for identifying conjugation sites that lead to an ADC with an optimized efficacy and safety profile may be warranted.

Materials and Methods

Cell lines

The cancer lines N87 (CRL-5822), BT474 (HTB-20), BT474-M1 (a subclone of BT474), HCC1954 (CRL-2338), SK-BR-3 (HTB-30), MDA-MB175-VII (HTB-25), MDA-MB468 (HTB-132), and MDA-MB-453 (HTB-131) were obtained from ATCC. The JIMT-1 line (17) was obtained from Deutsche Sammlung von Mikroorganismen und Zellkulturen, the German Collection of Microorganisms and Cell Cultures (DSMZ). MDA-MB361-DYT2 cline derived from metastatic breast carcinoma was a generous gift from Dr. Dajun Yang (Georgetown University, Washington, D.C.). Cell line growth conditions are available in Supplementary Data.

Generation and characterization of anti-HER2 antibodies and ADCs

Detailed anti-HER2 antibody and ADC generation and characterization are available in the Supplementary Data. Briefly, wild-type trastuzumab or engineered cysteine-mutant variants of trastuzumab were conjugated to smcc-DM1 or vc0101 via lysine or cysteines, respectively. A trastuzumab–maytansinoid conjugate produced at Pfizer, named "PT-DM1," comprised the Pfizer trastuzumab antibody covalently bound to the DM1 maytansinoid through the bifunctional linker, sulfosuccinimidyl 4-(N-maleimidomethyl) cyclohexane-1-carboxylate (sulfo-SMCC), and was prepared as described previously (4, 18). The DAR of PT-DM1 was determined to be in the range of 3.5–4.2. It is structurally similar to trastuzumab emtansine (T-DM1). A trastuzumab–auristatin conjugate, named "HER2-vc0101," comprised the Pfizer trastuzumab antibody covalently bound to the Aur0101 auristatin derivative via the valine-citrulline dipeptide linker, named "vc0101," through conventional cysteine conjugation methods. The average DAR of HER2-vc0101 was approximately 4. Site-specific conjugates of double-cysteine–mutant anti-HER2 antibodies were generated in a similar fashion. The DAR of the double-cysteine conjugates, including PF-06804103, was 4.

In vivo animal studies

All animal studies were approved by the Pfizer Institutional Animal Care and Use Committee according to established guidelines. Female NOD *scid* gamma (NSG, stock no.: 005557) were obtained from The Jackson Laboratory. Female athymic nude mice (nude, stock no.: 088) were obtained from Charles River Laboratories. The human patient-derived xenografts (PDX) were established from fragments of freshly resected breast tumors of CTG-0033 (clinically characterized as HER2 3+ by IHC) and 144580 [clinically characterized as triple-negative breast cancer (TNBC)] obtained in accordance with appropriate consent procedures. The breast PDXs were subcutaneously passaged *in vivo* as fragments from animal to animal in nude mice. The non–small cell lung cancer PDX model of 37622A1 has been described previously (19). In cell line xenograft (CLX) studies, nude mice were injected subcutaneously in the flank with suspensions of 1×10^6, 5×10^6, and 10×10^6 of N87, JIMT-1, and BT474 cells, respectively, in 50% Matrigel (BD Biosciences). Mice were randomized into study groups when tumors reached approximately 150–300 mm^3. Either PBS (Gibco, catalog no., 14190-144, as vehicle), PF-06804103, or PT-DM1 at different doses was administered intravenously starting on day 0 for a total of four doses, 4 days apart (four times every 4 days). Tumors were measured at least weekly with a Vernier caliper (Mitutoyo) and the tumor mass was calculated as volume = (width × width × length)/2.

Generation of an *in vivo* PT-DM1–resistant model

To generate PT-DM1–resistant tumors, nude mice were implanted subcutaneously with 7.5×10^6 N87 cells in 50% Matrigel (BD Biosciences). The animals were randomized into two groups when average tumor volume reached approximately 300 mm^3: (i) vehicle control ($n = 10$) and (ii) PT-DM1 treated ($n = 16$). PT-DM1 (6 mg/kg) or vehicle (PBS) was administered intravenously in saline on day 0 and

Published OnlineFirst August 3, 2020; DOI: 10.1158/1535-7163.MCT-20-0237

then the animals were dosed weekly with 6 mg/kg for 30 weeks. Most of the tumors responded to PT-DM1 treatment with reduction in tumor volume. When the individual tumor volume reached approximately 500 mm^3 (nearly double the original size of the tumor at randomization) while being dosed with PT-DM1, it was considered refractory or relapsed. The PT-DM1–resistant tumors were dosed with the PF-06804103 at 3 mg/kg weekly to evaluate its response *in vivo*.

Toxicity and toxicokinetic assessments of site-specific anti-HER2 ADCs in rats and nonhuman primates

All animal studies were approved by Pfizer Institutional Animal Care and Use Committees according to establish guidelines. Detailed animal information and experimental conditions are available in the Supplementary Data, as well as Supplementary Materials and Methods.

Results

Screening strategy for selection of optimal linker–payload conjugation sites for the anti-HER2 ADC, PF-06804103

To determine an ideal combination of sites that would yield a 4 DAR ADC with optimized physicochemical properties, we first evaluated a panel of single cysteine insertions and determined the conjugatability, stability, and hydrophobicity of the resulting ADC using the vc0101 linker–payload (9). The sites were chosen in the constant domain trastuzumab so as not to interfere with receptor binding, and the pKa of the installed sulfhydryl group was used as a measure of the relative solvent accessibility of this moiety for conjugation (**Fig. 1A**). Optimal properties for conjugatability and hydrophobicity of the resulting conjugate were chosen as a predicted pKa between 9.5 and 11.5 for the new sulfhydryl group and a side chain accessible surface area between 15 and 60 $Å^2$.

In addition, positions for cysteine mutagenesis were selected via peptide mapping of γ-calicheamicin conjugates wherein certain lysine (K) residues are preferred sites for conjugation. These four preferred lysine residues were K246, K290, K334, and K392 (EU numbering system as set forth in Kabat and colleagues, 1991, NIH Publication 91–3242, National Technical Information Service, Springfield, VA; https://www.worldcat.org/title/sequences-of-proteins-of-immunological-interest/oclc/24613501) in the human IgG1-Fc region and were selected as positions to engineer a reactive cysteine for site-specific conjugation to vc0101.

Sites that conjugated well to vc0101 were further evaluated for relative hydrophobicity as measured by retention time (RRT) on hydrophobic interaction chromatography (HIC; **Fig. 1B**). We

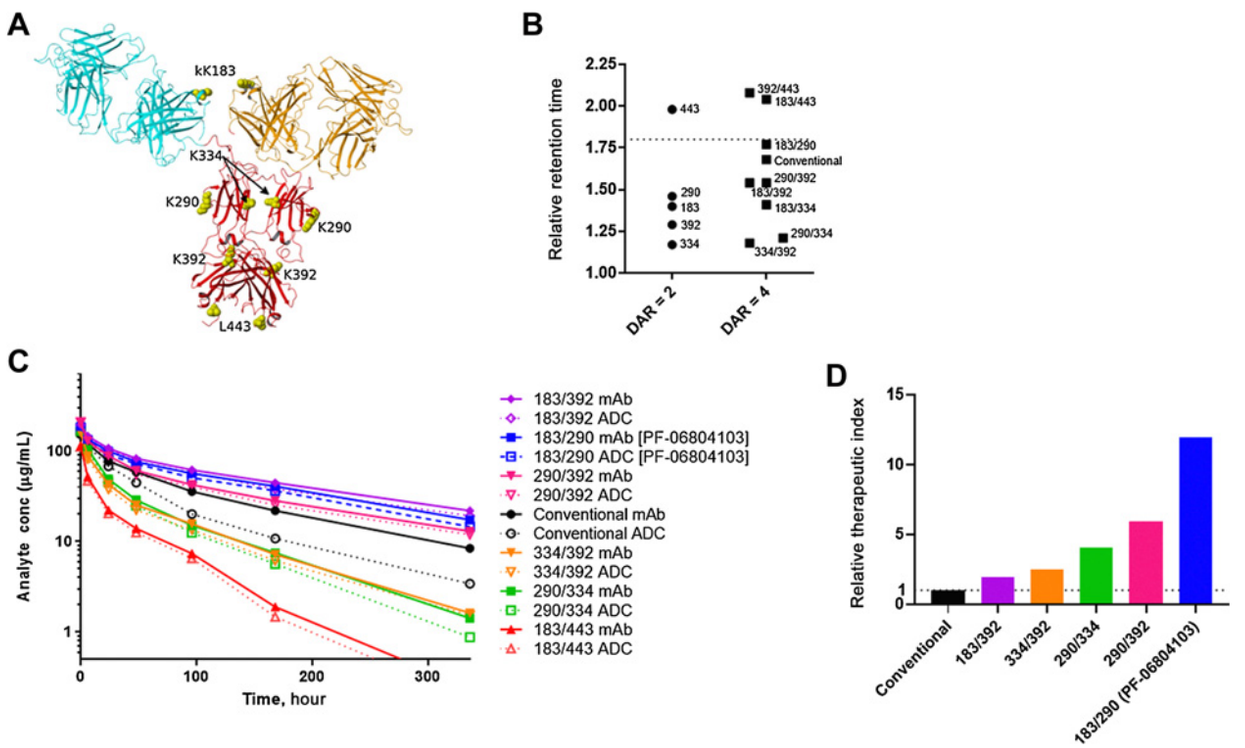

Figure 1.

Impact of different cysteine mutation sites on physiochemical and pharmacokinetic properties of anti-HER2 4 DAR vc0101 ADCs. **A,** Ribbon structure of trastuzumab overlaid with site locations of engineered cysteine mutations evaluated herein. **B,** ADC RRTs by HIC. The relative RRT was calculated as RRT of ADC divided by RRT of benchmark unconjugated wild-type trastuzumab having a typical RRT of 5.0–5.2 minutes. Circles, 2 DAR conjugates and squares, 4 DAR conjugates. Numbers next to data points represent locations of engineered cysteines at which the vc0101 linker payload was conjugated to each ADC. **C,** Single-dose pharmacokinetic analysis of conventional or site-specific anti-HER2 4 DAR vc0101 ADCs (at either 5 or 6 mg/kg) in cynomolgus monkeys. The total antibody curves are represented by the whole symbols connected by solid lines and the ADC curves are represented by hollowed symbols connected by dashed lines. The conventional and kK183C/L443C ADCs were dosed at 5 mg/kg, whereas all others were dosed at 6 mg/kg. **D,** The TI for each ADC was calculated and made relative to the TI of conventional conjugate. The TI was calculated as a ratio of ADC plasma exposure of a tolerated dose in cynomolgus monkey divided by ADC exposure of an efficacious dose in mice bearing N87 tumors. mAb, monoclonal antibody.

Published OnlineFirst August 3, 2020; DOI: 10.1158/1535-7163.MCT-20-0237

hypothesized that relative hydrophobicity could serve as a method for predicting steric accessibility of the linker–payload to metabolism and thus overall stability of the ADC in circulation (9). With the aim of identifying the best combination of single cysteine mutations to give a 4 DAR ADC, double mutants were conjugated with vc0101, and the hydrophobicity of the resulting ADCs was evaluated. Assuming an additive effect of conjugating a hydrophobic linker–payload to multiple sites, we predicted that double-cysteine–mutant ADCs employing the K334C site (single RRT = 1.17) should yield 4 DAR ADCs with the lowest HIC RRTs. This was in fact borne out by the observation that the ADCs with the lowest (approaching unity) RRTs were the combinations with K334C: K334C + K392C (RRT = 1.18), K290C + K334C (RRT = 1.21), and kK183C + K334C (RRT = 1.41). As expected, combinations with the L443C site produced much more hydrophobic ADCs: K392C + L443C (RRT = 2.08) and kK183C + L443C (RRT = 2.04).

To test the hypothesis that hydrophobicity determined by HIC RRT can predict pharmacokinetic behavior, we performed a single-dose pharmacokinetic analysis on a selection of the 4 DAR ADCs in cynomolgus monkeys (**Fig. 1C**; **Table 1**). As expected, all site-specific 4 DAR ADCs were more stable (ADC/antibody ratio ≥ 0.87) than the approximately 4 DAR conventional conjugate (ADC/antibody ratio = 0.66; **Table 1**). However, not all site-specific ADCs yielded higher serum ADC exposure than the conventional conjugate (**Fig. 1C**; **Table 1**). Surprisingly, the ADCs with the lowest RRTs (K334C + K392C and K290C + K334C) had among the least ADC exposure and shortest half-life among the 4 DAR ADCs tested. Interestingly, the kK183C + K290C ADC (henceforth named PF-06804103), which had an RRT = 1.77, was among the ADCs with the highest ADC exposure and longest half-life (**Table 1**). Despite these pharmacokinetic differences in cynomolgus monkeys, all the site-specific 4 DAR ADCs had similar antitumor efficacy in the N87 xenograft tumor model (Supplementary Fig. S1). Taken together, these data suggest that site-specific conjugation enhances *in vivo* ADC stability compared with a conventional conjugate and that other factors beyond hydrophobicity dictate the *in vivo* pharmacokinetic profile of ADCs.

We calculated the therapeutic index (TI, ratio of a toxic dose in cynomolgus monkeys compared with an efficacious dose in tumor-bearing mice) of these ADCs to determine which set of sites maximized the preclinical therapeutic window by incorporating various parameters including pharmacokinetics, efficacy, and safety (see Supplementary Data). All site-specific ADCs tested in these studies had a larger TI compared with the conventional conjugate (**Fig. 1D**). The site-specific conjugate containing the kK183C + K290C mutations (named PF-06804103) had the largest TI among the panel tested and was selected for further development.

Characterization of PF-06804103, a site-specific 4 DAR anti-HER2 ADC with a cleavable linker and permeable auristatin payload

As demonstrated by comparative HIC characterizations, the site-specific ADC, PF-06804103 (**Fig. 2A**), has a homogenous product profile when compared with the random lysine-conjugated ADC, PT-DM1 (**Fig. 2B**). Thus, the uniformity of PF-06804103's biophysical properties support smooth manufacturing and quality control for this product in a class of complex biomacromolecules.

T-DM1 is effective in tumor models and breast cancer patient tumors with high HER2 expression, but displays significantly reduced activity in tumor models and in patients with cancer with moderate and heterogeneous HER2 expression (20, 21). The two characteristics that contribute to this activity profile are potentially (i) the high recycling rate of HER2 and (ii) the membrane impermeability of the lysine-mcc-DM1–released species from T-DM1 (22, 23). To overcome the pharmacodynamic properties that limit T-DM1's efficacy, PF-06804103 utilizes an enzymatically cleavable di-peptide linker with a membrane permeable auristatin payload (vc0101). Independent of conjugation technique (conventional or site specific), HER2-targeted ADCs with the vc0101 linker–payload show enhanced potency to $HER2^+$ cell lines (e.g., N87, BT474, and MDA-MB175VII) as compared with PT-DM1 (**Fig. 2C**; Supplementary Table S2). Interestingly, in $HER2^-$ cell lines (HT29 and MDA-MB-468) ADCs with vc0101 exhibited less nonspecific activity than PT-DM1 (**Fig. 2C**; Supplementary Table S2). The conjugation of vc0101 did not alter the HER2-binding properties of PF-06804103 as compared with PT-DM1 or Herceptin (Supplementary Table S3).

PF-06804103 demonstrates bystander activity *in vivo*

Bystander activity is defined as the property of tumor-targeting therapeutics to affect not only $antigen^+$ tumor cells but neighboring

Table 1. Summary of Pharmacokinetic Parameters for Double-Cysteine Mutant Anti-HER2 ADCs in Sera of Non-Human Primates.

ADC	Dose (mg/kg)	Analyte	C_{max} (mg/mL)	AUC (0–inf) (μg-hour/mL)	$t_{1/2}$ (hour)	ADC/Ab ratio
Conventional	5	Total Ab	157	12,900	129	0.65
		ADC	154	8,280	107	
290/334	6	Total Ab	165	6,030	101	0.86
		ADC	163	5,160	77	
334/392	6	Total Ab	159	5,550	90	0.89
		ADC	157	4,950	87	
183/443	5	Total Ab	127	3,890	60[a]	0.87
		ADC	116	3,400	NC[b]	
183/392	6	Total Ab	195	23,600	162	0.90
		ADC	196	21,300	155	
290/392	6	Total Ab	205	15,900	142	0.92
		ADC	208	14,700	140	
183/290 (PF-06804103)	6	Total Ab	187	20,100	132	0.89
		ADC	181	17,900	125	

Abbreviation: Ab, antibody.
[a]Only $n = 1$.
[b]NC, not calculated (not enough measurable concentrations in terminal elimination phase to be able to calculate $t_{1/2}$).

Published OnlineFirst August 3, 2020; DOI: 10.1158/1535-7163.MCT-20-0237

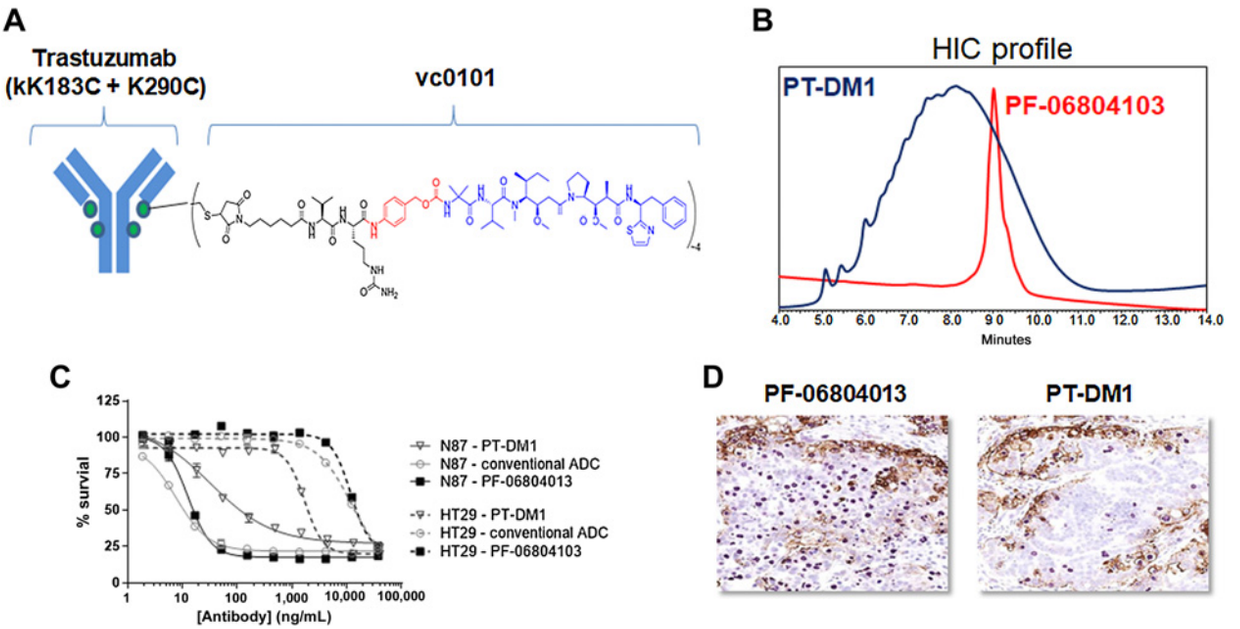

Figure 2.

PF-06804103 is a site-specific ADC employing a protease cleavable linker and membrane permeable auristatin payload. **A,** PF-06804103 is comprised of three components: (i) the trastuzumab-derived antibody, T-(kK183C+K290C), containing mutations of lysine to cysteine at the positions of kappa light chain constant region of K183 and Fc constant region of K290; (ii) a novel, potent auristatin payload, Aur-06380101, and (iii) an enzymatically cleavable linker, maleimidocaproyl-valine-citrulline, containing a p-aminobenzylcarbamate spacer. **B,** HIC profiles comparing the conventional lysine conjugate, PT-DM1, to the site-specific cysteine conjugate, PF-06804103. **C,** Cell viability assays were performed on HER2-positive (N87, solid lines) and HER2-negative (HT29, hashed lines) cell lines. **D,** Local bystander activity was assessed in N87 tumors following a single dose of T-DM1 or PF-06804103. Mice were perfused and tumors collected and formalin-fixed 24 hours after animals were dosed with the ADCs. Sections were immunostained for anti-HER2 antibody (brown) and pHH3 (purple).

antigen$^-$ tumor cells as well (24). PF-06804103 releases a membrane permeable auristatin, Aur0101, payload (16). To demonstrate the bystander activity of PF-06804103 *in vivo*, we dosed mice bearing HER2$^+$ N87 tumors with a single dose of PF-06804103 or PT-DM1 and collected the tumors 48 hours later. Immunostaining for human IgG revealed that PF-06804103 and PT-DM1 had similar tumor distribution (**Fig. 2D**). Utilizing a counterstain for phospho-histone H3 (pHH3), as a readout of mitotic arrest and surrogate pharmacodynamic marker of ADC efficacy, many of the ADC-bound tumor cells were pHH3$^+$ in tumors treated with either PF-06804103 or PT-DM1. Intriguingly, tumors treated with PF-06804103, as compared with PT-DM1, had more tumor cells that stained positive for pHH3, and, as a result of bystander activity *in vivo*, showed many more pHH3$^+$ cells distributed throughout the entire tumor section and not solely where the ADC was located. These findings suggest that the activity of the released auristatin was not confined to the tumor cells that were recognized by the ADC. Taken together, PF-06804103 is an ADC that utilizes a linker that abrogates the necessity for lysosomal localization and a payload with membrane penetration properties that mechanistically distinguishes PF-06804103 from T-DM1 and contributes to its enhanced pharmacodynamic properties.

PF-06804103 is more efficacious than PT-DM1 in breast cancer models

We evaluated the *in vivo* efficacy of PF-06804103 in T-DM1 eligible breast cancer tumor models. PDX-BRX-24312 and BT474-M1 are HER2-amplified tumors with high HER2 (HER2^{hi}) expression as assessed by IHC (Supplementary Fig. S2). Following a four times every 4 days dosing regimen, PF-06804103 showed better efficacy than PT-DM1 at similar dose levels (**Fig. 3A** and **B**). In both HER2^{hi} models, PF-06804103 treatment resulted in durable complete regressions that were sustained for >2 weeks after the last ADC dose. We next investigated the *in vivo* efficacy of PF-06804103 in T-DM1 ineligible breast cancer tumor models (e.g., non-HER2 amplified or tumors with low HER2 expression). PDX-BRX-11380 (from a patient with TNBC) and JIMT-1 (from a trastuzumab-refractory patient) are tumors with low HER2 expression (Supplementary Fig. S2). Utilizing a similar dosing regimen as above, PF-06804103 was more potent than PT-DM1 in these HER2^{lo} models (**Fig. 3C** and **D**). These data show that the enhanced pharmacodynamic properties of PF-06804103 translate into superior *in vivo* antitumor activity and suggest that PF-06804103 may be an effective therapeutic modality for patients with breast cancer.

PF-06804103 overcomes T-DM1 resistance

To determine whether PF-06804103 maintained its potency in the T-DM1–relapsed/refractory setting, we developed an *in vivo* model of PT-DM1 resistance in N87 tumors. HER2^{hi} N87 tumors regressed upon PT-DM1 dosing, but relapsed after drug withdrawal; however, PF-06804103 treatment resulted in sustained tumor regressions even after dosing cessation (**Fig. 3E**; Supplementary Fig. S1). To generate *in vivo* resistance, we treated N87 tumor–bearing mice with PT-DM1 on a weekly basis until the tumors relapsed on treatment (**Fig. 3F**). When each tumor reached approximately 500 mm^3 volume on PT-DM1 treatment, we switched the treatment to PF-06804103. After the first two PF-06804103 doses, all the PT-DM1–relapsed tumors regressed and shrank throughout

Published OnlineFirst August 3, 2020; DOI: 10.1158/1535-7163.MCT-20-0237

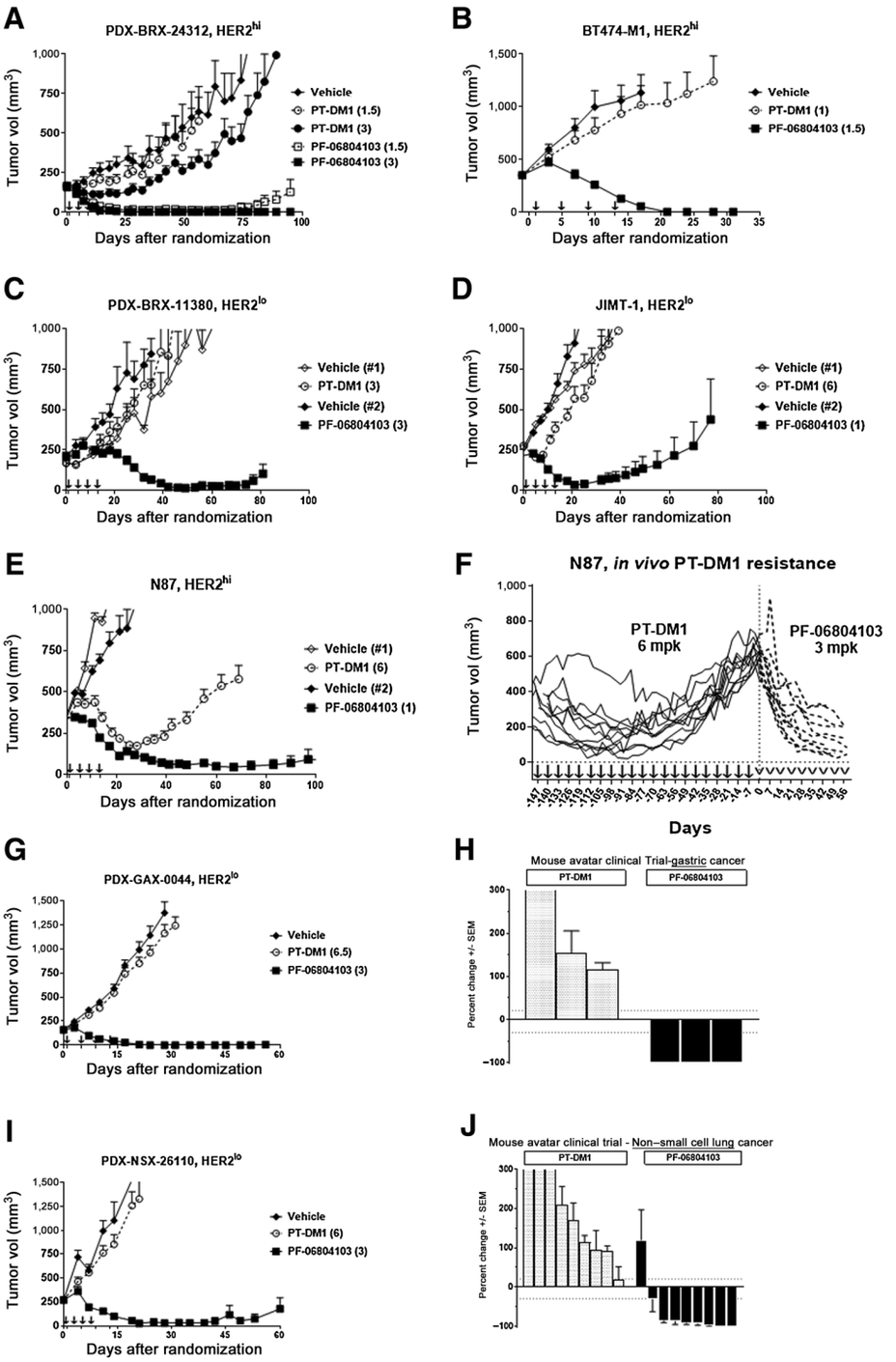

Figure 3.

PF-06804103 demonstrates superior *in vivo* antitumor efficacy compared with PT-DM1 in HER2-expressing breast, gastric, and lung cancer xenograft models. PDX (PDX-BRX-24312, **A**; PDX-BRX-11380, **B**; PDX-GAX-0044, **G**; and PDX-26110, **I**) and CLX (BT474-M1, **C**; JIMT-1, **D**; and N87, **E**) tumors were established in mice as described in the Materials and Methods, and were treated intravenously four times every four days with PBS as vehicle (diamonds), PT-DM1 (circles), or PF-06804103 (squares) at different doses (mg/kg). Data shown is the mean ± SEM of tumor size on each measurement day. **F,** Mice with N87 tumors were subjected to continuous weekly dosing with PT-DM1 at 6 mg/kg (solid lines, solid arrows) until tumor relapsed, at which point they were switched to weekly dosing with PF-06804103 at 3 mg/kg (dotted lines, open arrows; each line represents an individual mouse tumor followed over time, $n = 11$). **H** and **J,** Waterfall plots displaying mean best response per model, as calculated by % change from baseline, to four times every four days dosing of PT-DM1 (at 6 mg/kg; dashed boxes) or PF-06804103 (at 3 mg/kg; solid black bars). Error bars represent the SEM for each tumor model and treatment group. Arrows represent days when test agents were administered.

the duration of PF-06804103 treatment. Hence, PF-06804103 overcomes PT-DM1 resistance and may be an effective therapeutic modality in T-DM1–relapsed/refractory patients.

PF-068040103 demonstrates activity in HER2-expressing gastric and lung PDX models

Extending beyond breast cancer, HER2 overexpression is observed in a variety of solid tumors (e.g., gastric, non–small cell lung, etc.) and therapeutic targeting of HER2 has shown clinical benefit in some cases (e.g., trastuzumab in gastric cancer; refs. 25, 26). To determine whether PF-06804103 is effective in HER2-expressing nonbreast tumors, we evaluated the *in vivo* activity of PF-06804103 in a panel of HER2-expressing gastric (**Fig. 3G** and **H**; Supplementary Fig. S5) and non–small cell lung (**Fig. 3I** and **J**; Supplementary Fig. S2) cancer PDX models. In the PDX-GAX-0044 (**Fig. 3G**) and PDX-NSX-26110 (**Fig. 3I**) models, PF-06804103 resulted in sustained tumor regressions

Published OnlineFirst August 3, 2020; DOI: 10.1158/1535-7163.MCT-20-0237

as compared with PT-DM1. In a waterfall analysis across the panel of models tested, we calculated the best % change from baseline for each tumor to define an overall response rate (ORR) for PT-DM1 and PF-06804103. In the panel of gastric cancer PDX models, PF-06804103 and PT-DM1 had an ORR of three of three (100%) and zero of three (0%), respectively (**Fig. 3H**). In the panel of non–small cell lung cancer PDX models, PF-06804103 and PT-DM1 had an ORR of eight of nine (89%) and one of 10 (10%), respectively (**Fig. 3J**). Therefore, PF-06804103 showed promising *in vivo* activity in HER2-expressing nonbreast PDX models and may provide clinical benefit in HER2-expressing indications such as gastric and non–small cell lung cancer.

Significantly improved tolerability from bone marrow toxicity, stability, and exposure with PF-06804103 in rats and cynomolgus monkeys

The conventional, approximately 4 DAR conjugate (HER2-vc0101) and the site-specific conjugate, PF-06804103, were evaluated in exploratory and/or pivotal good laboratory practice-compliant repeat-dose toxicity studies in Sprague-Dawley rats and cynomolgus monkeys. In both species, the major toxicity with conventional HER2-vc0101 was reversible myelosuppression with associated hematologic changes. While bone marrow toxicity was still observed with PF-06804103, it was much less severe compared with that seen in animals administered an equivalent dose of HER2-vc0101.

In a repeat-dose toxicity study (three intravenous bolus doses, one dose/3 weeks), rats administered with 10 mg/kg/dose HER2-vc0101 showed marked decreases in bone marrow cellularity (**Table 2**). At 10 mg/kg/dose PF-06804103 in a similarly designed study (three intravenous bolus doses, one dose/3 weeks), rats exhibited minimal to moderate decreases in bone marrow cellularity, indicating that the site-specific conjugate caused less severe bone marrow toxicity compared with the conventional conjugate.

The most clinically relevant parameter to monitor myelosuppression and hematologic toxicities with anti-HER2 ADCs in cynomolgus monkeys was determined to be neutrophil counts. In repeat-dose toxicity studies in monkeys (three intravenous bolus doses, one dose/3 weeks), marked transient neutropenia (≤100 cells/μL) was seen with HER2-vc0101 at 5 mg/kg/dose, while only minimal effects on neutrophil counts were seen with PF-06804103 at 9 mg/kg/dose, demonstrating significant reduction of myelosuppression by site-specific conjugation (**Table 2**; **Fig. 4A**). Importantly, this alleviation was observed even with 4.5-fold higher ADC exposure for PF-06804103 at 9 mg/kg than the conventional conjugate at 5 mg/kg (**Fig. 4B**; **Table 2**, calculated by taking the ratio of ADC AUC for PF-06804103 by HER2-vc0101). Dose-limiting effects on neutrophils were observed at 12 mg/kg/dose with PF-06804103, resulting in early euthanasia of 3 of 6 males due to febrile neutropenia.

Microscopically, in the bone marrow of cynomolgus monkeys that survived to scheduled necropsy (3 days after the third dose), minimal to mild increased myeloid/erythroid (M/E) ratio was seen with conventional HER2-vc0101 at ≥3 mg/kg, with all animals (2/2) at 5 mg/kg having mild severity. Increased M/E ratio was described as decreased erythroid precursors combined with an increase of primarily mature granulocytes. This finding is consistent with bone marrow toxicity and an early regenerative response. In animals administered with PF-06804103, minimal to mild increased M/E ratio was seen starting at 6 mg/kg, with approximately half of the animals at 12 mg/kg having mild severity. When comparing the incidence and severity of this microscopic finding at similar doses of 5 mg/kg HER2-vc0101 and 6 mg/kg PF-06804103 (**Table 2**), there was a higher percentage of animals (100%) with a mild increase of M/E ratio administered with HER2-vc0101 compared with animals administered with 6 mg/kg PF-06804103 that had minimal (38%) or mild (13%) increase of M/E ratios. Again, this indicates an alleviation of myelosuppression by site-specific conjugation.

Table 2. Summary of clinically tolerated doses and effects on indicators of bone marrow toxicity in rats and monkeys.

Parameter	HER2-vc0101 Conventional DAR=4		PF-06804103 Site-specific DAR=4	
Sprague-Dawley rats [repeat-dose studies (3 doses, q3w)]				
Incidence of decreased bone marrow cellularity in repeat-dose studies (3 doses, q3w) on day 46	10 mg/kg		10 mg/kg	
Minimal	—		2/6	
Mild	—		1/6	
Moderate	—		3/6	
Marked	5/5		—	
Cynomolgus monkeys [repeat-dose studies (3 doses, q3w)]				
Highest clinically tolerated dose	5 mg/kg		9 mg/kg	
ADC AUC (0–inf) (μg-h/mL)	8,280		380,00	
ADC $t_{1/2}$ (h)	107		167	
Range of postdose WBC or NEUT cell count (10^3 cells/μL) nadirs in individual animals	WBC	NEUT	WBC	NEUT
0 mg/kg	6.8–14.2	1.61–7.39 (0/14)[a]	6.8–14.2	1.61–7.39 (0/14)[a]
3 mg/kg	5.6–12.8	0.39–2.88 (0/2)[a]	4.8–8.5	1.25–2.42 (0/6)[a]
5 mg/kg	1.3–3.7	0.00–0.04 (2/2)[a]	NA	NA
6 mg/kg	NA	NA	5.6–10.9	0.73–3.22 (0/8)[a]
9 mg/kg	NA	NA	6.8–9.4	0.9.-0.95 (0/2)[a]
12 mg/kg	NA	NA	1.8–11.0	0.02–4.25 (4/12)[a]
Incidence of increased M/E ratio in the bone marrow on day 46	5 mg/kg		6 mg/kg	
Minimal	—		3/8	
Mild	2/2		1/8	

Abbreviations: —, no finding; NA, not applicable; NEUT, neutrophils; q3w, 1 dose every 3 weeks; WBC, white blood cells.
[a]Incidence of animals with neutrophil counts below 100 cells/μL.

Published OnlineFirst August 3, 2020; DOI: 10.1158/1535-7163.MCT-20-0237

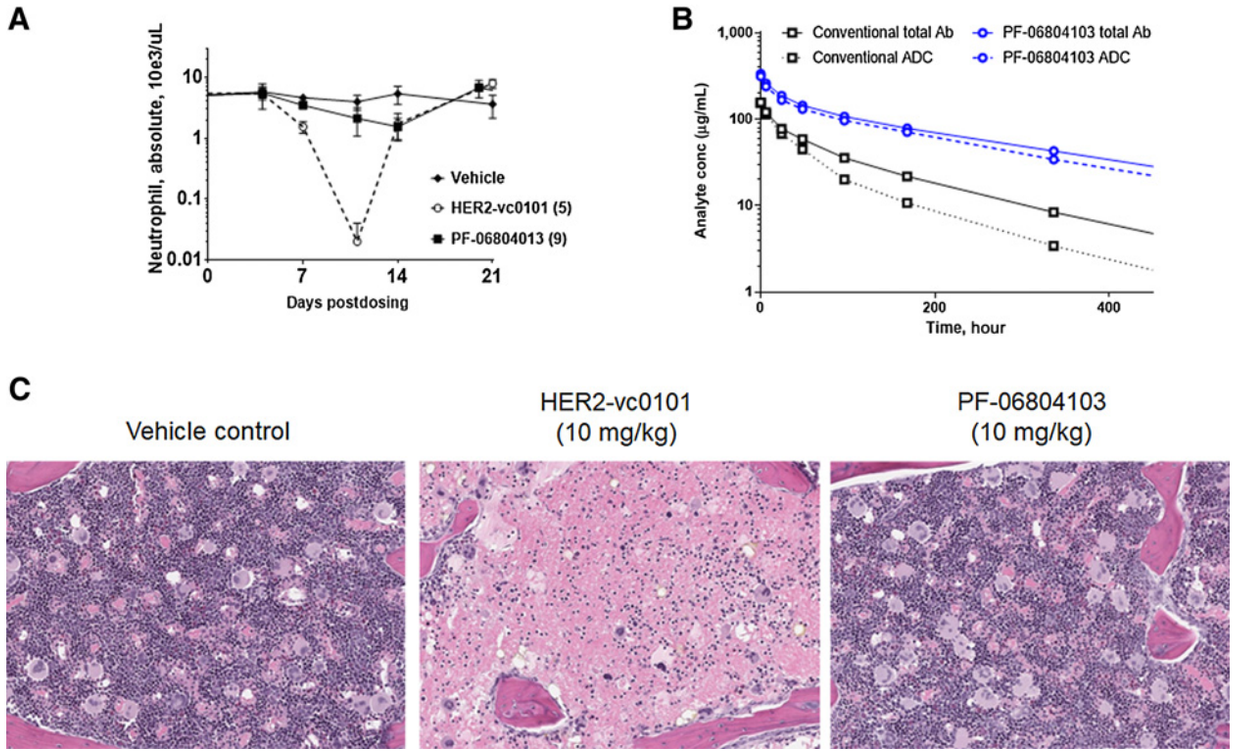

Figure 4.

Site-specific conjugation employed, PF-06804103, alleviates myelosuppression observed by conventional HER2-vc0101 conjugate. **A,** Cynomolgus monkeys were administered a single dose of HER2-vc0101 (5 mg/kg) or PF-06804103 (9 mg/kg) followed by a blood draw and neutrophil count in a time course up to 21 days after dosing. **B,** Toxicokinetic assessment of single dose HER2-vc0101 (5 mg/kg, squares) and PF-06804103 (9 mg/kg, circles) in cynomolgus monkeys. Solid lines, measured conjugated antibody and hashed lines, measured unconjugated antibody. **C,** Male rats were administered vehicle or 10 mg/kg HER2-vc0101 or PF-06804103 by intravenous bolus injection and then necropsied after 4 days. Representative bone marrow sections stained with hematoxylin and eosin following necropsy at 20× magnification are shown.

One potential explanation for the less severe bone marrow toxicity observed with the site-specific conjugate, PF-06804103, was the reduced payload loss seen with this molecule compared with the conventional conjugate, HER2-vc0101. To assess this hypothesis, we compared the severity of bone marrow toxicity and plasma concentration of free payload in rats dosed with HER2-vc0101 and PF-06804103 at 10 mg/kg. As observed in cynomolgus monkeys, PF-06804103 had higher ADC and less free payload exposure in the serum in rats dosed at 10 mg/kg of each ADC (Supplementary Table S4). In addition, PF-06804103 abrogated the hematology changes and alleviated the decreases in bone marrow cellularity in these rats as compared with those dosed with HER2-vc0101 (**Fig. 4C**; Supplementary Table S4).

To further investigate the contribution of the payload to the observed bone marrow toxicity, rats were continuously intravenously infused with the Aur0101 payload for 72 hours or, as a control, administered with HER2-vc0101 by intravenous bolus injection at levels that would produce similar exposure profiles for Aur0101. At 171.5 µg/kg Aur0101 payload or 10 mg/kg ADC, rats exhibited marked bone marrow toxicity at 72 hours postdose (Supplementary Table S5). At the lower doses of the payload and ADC, the incidence and severity of the bone marrow toxicity were only slightly greater with the ADC at 3 mg/kg compared with the payload at 51.5 µg/kg. These data demonstrate that systemic administration of the payload alone causes similar bone marrow toxicity to that seen with the conventional ADC.

Discussion

The approval of T-DM1 validated that the targeted delivery of chemotherapeutics via the ADC modality could be effective in solid tumors. As a standard-of-care second-line treatment option for patients with HER2-positive breast cancer, T-DM1 has improved the care of these patients. Yet, design improvements to this first-generation ADC could lead to a more efficacious and better tolerated treatment option. Because HER2 is expressed in multiple tumor types, the scope of potential treatable indications could be greatly widened by targeting low and heterogeneously HER2-expressing cancers. T-DM1 is primarily efficacious in patients with very high and homogenously HER2-expressing breast cancers. Moreover, in patients that respond to T-DM1, acquired resistance to T-DM1 remains a problem for patients that progress on treatment. Therefore, the primary rationale for designing an improved HER2-targeting ADC was to improve efficacy against tumors with low HER2 expression, demonstrate efficacy in tumors resistant to T-DM1, and improve the safety profile by reducing off-target toxicity associated with cleavable linkers and microtubule inhibitor payloads.

Published OnlineFirst August 3, 2020; DOI: 10.1158/1535-7163.MCT-20-0237

The mechanism of action for T-DM1 requires ADC binding to HER2, internalization, trafficking to the lysosome, release of the payload in the lysosome, and shuttling of the payload from the lysosomal lumen into the cytoplasmic space. Given the recycling rate of internalized HER2 back to the plasma membrane, it is estimated that approximately 10% of T-DM1 that binds to the surface of a HER2-expressing cancer cell delivers its payload into the cytoplasmic space (22, 23). To maximize payload delivery efficiency, PF-06804103 utilizes the protease cleavable valine-citrulline linker with an auristatin analogue, auristatin-0101, rationally designed for optimal microtubule inhibition and membrane permeability. This linker–payload combination enables PF-06804103 to kill HER2-expressing cells as well as neighboring cells regardless of HER2 expression ("bystander activity"). Bystander activity is a key attribute engineered into the designs of a new generation of anti-HER2 ADCs (e.g., PF-06804103, SYD985, MEDI4276, DS8201a, etc.) that improves their efficacy profiles compared with T-DM1. Driven by the enhanced payload delivery afforded by the cleavable linker, PF-06804103 demonstrates broader antitumor activity compared with T-DM1 in a panel of CLXs and PDXs including those with low and heterogeneous HER2 expression patterns. This linker–payload combination also enables PF-06804103 to overcome T-DM1 resistance. In our model of *in vivo* T-DM1 resistance, PF-06804103 was able to shrink T-DM1 refractory tumors that continued to express HER2 (Supplementary Fig. S2). Interestingly, these T-DM1 refractory tumors were also enriched for caveolin-1 protein, which may mediate caveolar ADC endocytosis as an antigen-independent mechanism of resistance to T-DM1 (27).

We set out to create a site-specific 4 DAR conjugate; however, this required empirical evaluation of conjugation of vc0101 to cysteine mutations in the antibody backbone (9). Point insertions of cysteine in the antibody framework have previously been shown to confer stability advantages when conjugating reactive electrophiles (i.e., maleimides) at some residues but not others (8, 28, 29). We, therefore, designed mutant antibodies with cysteine point insertions into the constant region at specific sites such that: (i) they would preserve antibody folding, expression, stability, or solubility; (ii) the change would retain antibody functional properties including antigen binding, Fcγ receptor binding, and FcRn binding; (iii) the resulting thiol would have partial solvent exposure on the basis of predicted pKa and side chain accessible surface area; and (iv) provide high plasma stability. As a guide to improving plasma stability, we observed that ADCs employing vc0101 at different sites exhibited remarkably different HIC RRTs. We and others have hypothesized that increased RRT could be a result of increased surface lipophilicity on the ADC, and may lead to pharmacokinetics divergent from wild-type antibody such that a relative HIC RRT equal to one is desirable (9). To achieve a 4 DAR conjugate with optimized *in vivo* serum exposure, we, therefore, evaluated cysteine-mutant combinations that gave rise to low relative HIC scores, with the aim of increasing ADC stability and exposure in nonhuman primates. Surprisingly, two ADCs with low HIC scores showed poor exposure in cynomolgus monkeys. To test this hypothesis further, we evaluated the kK183C/K290C combination with vc0101; the relative HIC retention of 1.77 predicted a lower exposure than wild-type antibody, however, the opposite was observed. The kK183C/K290C ADC (PF-06804103) had improved exposure in cynomolgus monkeys, relative to both K334C/K392C and K290C/K334C ADCs. This result suggests that HIC RRT alone is insufficient to predict pharmacokinetics for these ADCs, and that other factors (e.g., FcRn binding) may also play a role in governing ADC exposure *in vivo*. In addition, we found that certain sites led to ADCs with poor ADC exposure in cynomolgus monkeys (e.g., K334 and L443). We imply by these data that the engineered cysteines at K183/L443 and/or the conjugation of them to the vc0101 linker–payload yields an antibody or ADC that clears much more quickly in cynomolgus monkey than an antibody or ADC without these specific mutations and conjugations at them. These data highlight the importance of selecting the right sites when optimizing the pharmacologic attributes of a site-specific ADC.

Clinically, the ADCs that are conventional conjugates with the same linker–payload class as PF-06804103 (cleavable linker with microtubule inhibitor payload), have similar MTDs driven by common off-target DLTs, such as neutropenia, which are independent of the target antigen or conjugate antibody and may be mediated by conjugate instability (6). We hypothesized that by increasing the stability of the vc0101 linker–payload by the site-specific conjugation designed into PF-06804103, we could generate a molecule with better serum stability to overcome the myelosuppression observed by conventional conjugates. When the site-specific conjugate, PF-06804103, was evaluated in rats and monkeys in repeat-dose toxicity studies, it showed an improved bone marrow safety profile along with higher serum exposures resulting in an overall better therapeutic window when compared with the conventional conjugate, HER2-vc0101. This improvement was primarily attributed to the enhanced stability of the site-specific conjugate. Our hypothesis was supported by an experiment which showed that rats administered with HER2-vc0101, which produced higher systemic concentrations of free payload (i.e., less stable), had greater changes in biomarkers of bone marrow toxicity as compared with PF-06804103. Furthermore, when the Aur0101 payload alone was administered to rats, similar levels of bone marrow toxicity were observed compared with HER2-vc0101 doses, which produced a similar systemic Aur0101 exposure profile. Thus, PF-06804103 was tolerated at higher doses in rats and nonhuman primates and showed less severe myelosuppression and bone marrow toxicity compared with the conventional HER2-vc0101 conjugate when equivalent doses were evaluated.

In summary, we created PF-06804103, a unique site-specific anti-HER2 ADC that has (i) improved potency over T-DM1, (ii) the ability to overcome T-DM1 resistance, (iii) optimized pharmacokinetic properties, and (iv) site-specific conjugation resulting in enhanced ADC stability that mitigates myelosuppression and increases the clinically tolerated dose in nonhuman primates compared with a conventional conjugate in nonclinical toxicology assessments. If these preclinical data translate into the clinical setting, this ADC holds the potential to be a transformative new therapy for patients with cancer with HER2-expressing tumors. PF-06804103 is currently under clinical investigation (NCT03284723).

Disclosure of Potential Conflicts of Interest

E.I. Graziani reports personal fees from Pfizer Inc. (employee) outside the submitted work and has a patent for WO2017/093844 pending. M. Sung reports personal fees from Pfizer Inc. (employee) outside the submitted work. K. Marquette reports personal fees from Pfizer Inc. (employee) outside the submitted work and has a patent for WO2017/093844 pending. S. Puthenveetil reports personal fees from Pfizer Inc (past employee) during the conduct of the study. J. Bikker reports personal fees from Pfizer Inc. (employee at time research conducted) outside the submitted work. J. Casavant reports personal fees from Pfizer Inc. (employee) outside the submitted work. E.M. Bennett reports personal fees from Pfizer Inc. (employee) outside the submitted work and has a patent for EP2794653B1 issued. M.B. Charati reports personal fees from Pfizer Inc. (employee) outside the submitted work. C. Hosselet reports personal fees from Pfizer, Inc. (employee) outside the submitted work. M. Finkelstein reports other from Pfizer (employee) during the conduct of the study and outside the submitted work. T. Clark reports personal fees from Pfizer Inc. (employee) outside the submitted work. F. Barletta reports other from Pfizer (employed by Pfizer and owns Pfizer stock) outside the submitted work. E. Rosfjord

reports personal fees from Pfizer Inc. (full-time employee) outside the submitted work. F. Loganzo reports personal fees from Pfizer (employee) outside the submitted work and has a patent for WO2017/093844 pending. C.J. O'Donnell reports personal fees from Pfizer Inc. (employee) outside the submitted work. P. Sapra reports personal fees from Pfizer Inc. (employee) outside the submitted work and has a patent for WO2017/093844 pending. No potential conflicts of interest were disclosed by the other authors.

Authors' Contributions

E.I. Graziani: Conceptualization, resources, data curation, formal analysis, visualization, writing-original draft, project administration. **M. Sung:** Conceptualization, resources, data curation, formal analysis, investigation, visualization, methodology, writing-original draft, project administration, writing-review and editing. **D. Ma:** Conceptualization, data curation, visualization, writing-original draft, project administration. **B. Narayanan:** Resources, investigation, methodology. **K. Marquette:** Conceptualization, resources, investigation. **S. Puthenveetil:** Resources. **L.N. Tumey:** Conceptualization, resources. **J. Bikker:** Resources. **J. Casavant:** Resources. **E.M. Bennett:** Resources, software, visualization. **M.B. Charati:** Resources, investigation, visualization. **J. Golas:** Resources, investigation, visualization. **C. Hosselet:** Resources, data curation, investigation, methodology. **C.M. Rohde:** Conceptualization, data curation, formal analysis, investigation, visualization, writing-original draft, writing-review and editing. **G. Hu:** Resources, investigation, methodology. **M. Guffroy:** Conceptualization, resources, data curation, investigation, methodology. **H. Falahatpisheh:** Conceptualization, resources, data-curation, methodology. **M. Finkelstein:** Conceptualization, supervision, funding acquisition, writing-review and editing. **T. Clark:** Resources, data curation, formal analysis, investigation. **F. Barletta:** Conceptualization, data curation, formal analysis, investigation, visualization, writing-review and editing. **L. Tchistiakova:** Conceptualization, supervision, funding acquisition. **J. Lucas:** Conceptualization, supervision. **E. Rosfjord:** Conceptualization, supervision, methodology, writing-review and editing. **F. Loganzo:** Conceptualization, data curation, software, supervision, writing-review and editing. **C.J. O'Donnell:** Conceptualization, supervision, funding acquisition, writing-review and editing. **H.-P. Gerber:** Conceptualization, supervision, funding acquisition. **P. Sapra:** Conceptualization, supervision, funding acquisition, writing-review and editing.

Acknowledgments

We would like to acknowledge contributions by the PF-06804103 Project Team, including but not limited to Harman Dube, Ira Jacobs, Steve Max, Brian Kennedy, Haige Zhang, Mike Cinque, Kenny Kim, Jessica Kearney, Bryan Peano, Johnny Yao, Elwira Muszynska, Nadira Prashad, Sylvia Musto, Xingzhi Tan, My-Hanh Lam, Xiang Zheng, Kiran Khandke, Guixian Jin, Xiaogang Han, Alison Betts, Nahor Haddish-Berhane, Laurie Tylaska, Lindsay King, Russell Dushin, Andreas Maderna, Chakrapani Subramanyam, Jennifer Thorn, Frank Kotch, Birte Nolting, Amar Prashad, April Xu, Shuntai Wang, and Mark Kaplan.

The costs of publication of this article were defrayed in part by the payment of page charges. This article must therefore be hereby marked *advertisement* in accordance with 18 U.S.C. Section 1734 solely to indicate this fact.

Received March 26, 2020; revised June 4, 2020; accepted July 14, 2020; published first August 3, 2020.

References

1. Beck A, Goetsch L, Dumontet C, Corvaia N. Strategies and challenges for the next generation of antibody-drug conjugates. Nat Rev Drug Discov 2017;16:315–37.
2. Chari RV. Expanding the reach of antibody-drug conjugates. ACS Med Chem Lett 2016;7:974–6.
3. Coats S, Williams M, Kebble B, Dixit R, Tseng L, Yao NS, et al. Antibody-drug conjugates: future directions in clinical and translational strategies to improve the therapeutic index. Clin Cancer Res 2019;25:5441–8.
4. Lambert JM, Chari RV. Ado-trastuzumab Emtansine (T-DM1): an antibody-drug conjugate (ADC) for HER2-positive breast cancer. J Med Chem 2014;57:6949–64.
5. Francisco JA, Cerveny CG, Meyer DL, Mixan BJ, Klussman K, Chace DF, et al. cAC10-vcMMAE, an anti-CD30-monomethyl auristatin E conjugate with potent and selective antitumor activity. Blood 2003;102:1458–65.
6. Hinrichs MJ, Dixit R. Antibody drug conjugates: Nonclinical safety considerations. AAPS J 2015;17:1055–64.
7. Junutula JR, Raab H, Clark S, Bhakta S, Leipold DD, Weir S, et al. Site-specific conjugation of a cytotoxic drug to an antibody improves the therapeutic index. Nat Biotechnol 2008;26:925–32.
8. Tian F, Lu Y, Manibusan A, Sellers A, Tran H, Sun Y, et al. A general approach to site-specific antibody drug conjugates. Proc Natl Acad Sci U S A 2014;111:1766–71.
9. Tumey LN, Li F, Rago B, Han X, Loganzo F, Musto S, et al. Site selection: a case study in the identification of optimal cysteine engineered antibody drug conjugates. AAPS J 2017;19:1123–35.
10. Yan M, Schwaederle M, Arguello D, Millis SZ, Gatalica Z, Kurzrock R. HER2 expression status in diverse cancers: review of results from 37,992 patients. Cancer Metastasis Rev 2015;34:157–64.
11. Rinnerthaler G, Gampenrieder SP, Greil R. HER2 directed antibody-drug-conjugates beyond T-DM1 in breast cancer. Int J Mol Sci 2019;20;1115.
12. Dokter W, Ubink R, van der Lee M, van der Vleuten M, van Achterberg T, Jacobs D, et al. Preclinical profile of the HER2-targeting ADC SYD983/SYD985: introduction of a new duocarmycin-based linker-drug platform. Mol Cancer Ther 2014;13:2618–29.
13. Humphreys RC, Kirtely J, Hewit A, Biroc S, Knudsen N, Skidmore L, et al. Site specific conjugation of ARX-788, an antibody drug conjugate (ADC) targeting HER2, generates a potent and stable targeted therapeutic for multiple cancers. In: Proceedings of the 106th Annual Meeting of the American Association for Cancer Research; 2015 Apr 18–22; Philadelphia, PA. Philadelphia (PA): AACR; 2015. Abstract nr 639.
14. Li JY, Perry SR, Muniz-Medina V, Wang X, Wetzel LK, Rebelatto MC, et al. A biparatopic HER2-targeting antibody-drug conjugate induces tumor regression in primary models refractory to or ineligible for HER2-targeted therapy. Cancer Cell 2016;29:117–29.
15. Ogitani Y, Aida T, Hagihara K, Yamaguchi J, Ishii C, Harada N, et al. DS-8201a, a novel HER2-targeting ADC with a novel DNA topoisomerase I inhibitor, demonstrates a promising antitumor efficacy with differentiation from T-DM1. Clin Cancer Res 2016;22:5097–108.
16. Maderna A, Doroski M, Subramanyam C, Porte A, Leverett CA, Vetelino BC, et al. Discovery of cytotoxic dolastatin 10 analogues with N-terminal modifications. J Med Chem 2014;57:10527–43.
17. Tanner M, Kapanen AI, Junttila T, Raheem O, Grenman S, Elo J. Characterization of a novel cell line established from a patient with Herceptin-resistant breast cancer. Mol Cancer Ther 2004;3:1585–92.
18. Chari R, Martell BA, Gross JL, Cook SB, Shah SA, Blattler WA. Immunoconjugates containing novel maytansinoids: promising anticancer drugs. Cancer Res 1992;52:127–31.
19. Damelin M, Geles KG, Follettie MT, Yuan P, Baxter M, Golas J, et al. Delineation of a cellular hierarchy in lung cancer reveals an oncofetal antigen expressed on tumor-initiating cells. Cancer Res 2011;71:4236–46.
20. Yamashita-Kashima Y, Shu S, Harada N, Fujimoto-Ouchi K. Enhanced antitumor activity of trastuzumab emtansine (T-DM1) in combination with pertuzumab in a HER2-positive gastric cancer model. Oncol Rep 2013;30:1087–93.
21. Perez EA, Hurvitz SA, Amler LC, Mundt KE, Ng V, Guardino E, et al. Relationship between HER2 expression and efficacy with first-line trastuzumab emtansine compared with trastuzumab plus docetaxel in TDM4450g: a randomized phase II study of patients with previously untreated HER2-positive metastatic breast cancer. Breast Cancer Res 2014;16:R50.
22. Austin CD, De Maziere AM, Pisacane PI, van Dijk SM, Eigenbrot C, Sliwkowski MX, et al. Endocytosis and sorting of ErbB2 and the site of action of cancer therapeutics trastuzumab and geldanamycin. Mol Biol Cell 2004;15:5268–82.
23. Kovtun YV, Audette CA, Ye Y, Xie H, Ruberti MF, Phinney SJ, et al. Antibody-drug conjugates designed to eradicate tumors with homogeneous

Published OnlineFirst August 3, 2020; DOI: 10.1158/1535-7163.MCT-20-0237

and heterogeneous expression of the target antigen. Cancer Res 2006;66: 3214–21.
24. Li F, Emmerton KK, Jonas M, Zhang X, Miyamoto JB, Setter JR, et al. Intracellular released payload influences potency and bystander-killing effects of antibody-drug conjugates in preclinical models. Cancer Res 2016;76:2710–9.
25. Martin V, Cappuzzo F, Mazzucchelli L, Frattini M. HER2 in solid tumors: more than 10 years under the microscope; where are we now? Future Oncol 2014;10: 1469–86.
26. Bang YJ, Van Cutsem E, Feyereislova A, Chung HC, Shen L, Sawaki A, et al. Trastuzumab in combination with chemotherapy versus chemotherapy alone for treatment of HER2-positive advanced gastric or gastro-oesophageal junction cancer (ToGA): a phase 3, open-label, randomised controlled trial. Lancet 2010; 376:687–97.
27. Sung M, Tan X, Lu B, Golas J, Hosselet C, Wang F, et al. Caveolae-mediated endocytosis as a novel mechanism of resistance to trastuzumab emtansine (T-DM1). Mol Cancer Ther 2018;17:243–53.
28. Pillow TH, Tien J, Parsons-Reponte KL, Bhakta S, Li H, Staben LR, et al. Site-specific trastuzumab maytansinoid antibody-drug conjugates with improved therapeutic activity through linker and antibody engineering. J Med Chem 2014; 57:7890–9.
29. Junutula JR, Bhakta S, Raab H, Ervin KE, Eigenbrot C, Vandlen R, et al. Rapid identification of reactive cysteine residues for site-specific labeling of antibody-Fabs. J Immunol Methods 2008;332:41–52.

AACR American Association for Cancer Research

Molecular Cancer Therapeutics

PF-06804103, A Site-specific Anti-HER2 Antibody–Drug Conjugate for the Treatment of HER2-expressing Breast, Gastric, and Lung Cancers

Edmund I. Graziani, Matthew Sung, Dangshe Ma, et al.

Mol Cancer Ther 2020;19:2068-2078. Published OnlineFirst August 3, 2020.